

## On two distinct types of drag-reducing fluids, diameter scaling, and turbulent profiles

K. Gasljevic, G. Aguilar, E.F. Matthys\*

*Department of Mechanical and Environmental Engineering, University of California at Santa Barbara,  
Santa Barbara, CA 93106, USA*

Received 29 October 1999; received in revised form 17 August 2000

---

### Abstract

Two distinct scaling procedures were found to predict the diameter effect for different types of drag-reducing fluids. The first one, which correlates the relative drag reduction (DR) with flow bulk velocity ( $V$ ), appears applicable to fluids that comply with the 3-layers velocity profile model. This model has been applied to many polymer solutions; but the drag reduction versus  $V$  scaling procedure was successfully tested here for some surfactant solutions as well. This feature, together with our temperature profile measurements, suggest that these surfactant solutions may also show this type of 3-layers velocity profiles (3L-type fluids).

The second scaling procedure is based on a correlation of  $\tau_w$  versus  $V$ , which is found to be applicable to some surfactant solutions but appears to be applicable to some polymer solutions as well. The distinction between the two procedures is therefore not simply one between polymer and surfactants. It was also seen that the  $\tau_w$  versus  $V$  correlation applies to fluids which show a stronger diameter effect than those scaling with the other procedure. Moreover, for fluids that scale according to the  $\tau_w$  versus  $V$  procedure, the drag-reducing effects extend throughout the whole pipe cross section even at conditions close to the onset of drag reduction, in contrast to the behavior of 3L fluids. This was shown by our measurements of temperature profiles which exhibit a fan-type pattern for the  $\tau_w$  versus  $V$  fluids (F-type), unlike the 3-layers profile for the fluids well correlated by drag reduction versus  $V$ . Finally, mechanically-degraded polymer solutions appeared to behave in a manner intermediate between the 3L and F fluids.

Furthermore, we also showed that a given fluid in a given pipe may transition from a Type A drag reduction at low Reynolds number to a Type B at high Reynolds number, the two types apparently being more representative of different levels of fluid/flow interactions than of fundamentally different phenomena of drag reduction. After transition to the non-asymptotic Type B regime, our results suggest that, without degradation, the friction becomes independent of pipe diameter and that the drag reduction level becomes also approximately independent of the Reynolds number, in a strong analogy to Newtonian flow. © 2001 Elsevier Science B.V. All rights reserved.

*Keywords:* Drag reduction; Diameter effect; Scaling; Turbulence; Temperature profiles; Surfactants; Polymers; Newtonian flow; Reynolds number

---

\* Corresponding author.

**Nomenclature**

$C_F = 2\tau_w/\rho V^2$	friction coefficient
$C_p$	heat capacity ( $\text{J kg}^{-1} \text{K}^{-1}$ )
$DR = (1 - C_F/C_{F,S}) \times 100$	drag reduction level (%)
$q_w''$	heat flux at the wall ( $\text{W m}^{-2}$ )
$Re = VD/\nu$	Reynolds number
$T^+ = (T_w - T)u^*\rho C_p/q_w''$	dimensionless wall-to-local temperature difference
$u^* = \sqrt{\tau_w/\rho}$	shear velocity ( $\text{m s}^{-1}$ )
$V$	bulk velocity ( $\text{m s}^{-1}$ )
$y$	distance from the wall (m)
$y^+ = yu^*/\nu$	dimensionless distance from the wall

*Greek letters*

$\nu$	kinematic viscosity ( $\text{m}^2 \text{s}^{-1}$ )
$\rho$	density ( $\text{kg m}^{-3}$ )
$\tau_w$	shear stress at the wall ( $\text{N m}^{-2}$ )

*Subscripts*

a	apparent
S	solvent (water)
w	wall

**1. Introduction**

It is well known that the presence in water of small amounts of certain additives (such as polymers or surfactants) can result in a considerable reduction of drag in turbulent flow. One of many interesting aspects of these drag-reducing flows is the so-called ‘diameter effect’. This effect is seen as the additional dependence of the friction coefficient ( $C_F$ ) on the pipe diameter, in addition to the dependence on the Reynolds number which is the only parameter needed to define the friction coefficient for Newtonian fluids in smooth pipes.

In a recent study [1], we addressed the diameter effect on polymeric drag-reducing fluids and proposed a scaling procedure which proved to be very simple and accurate. We showed that the drag reduction level is better correlated by the flow bulk velocity ( $V$ ) than by other more complicated parameters proposed earlier. Our analysis also showed that this scaling procedure ties in very well with Virk’s 3-layers model [2] which was experimentally found to fit most polymer solutions; and that the thickness of the elastic layer (as defined by the  $\Delta B^+$  displacement of the Newtonian core) is better defined as a function of  $V$  than of  $\tau_w$  or  $u^*$ , as previously believed. This suggests that solutions which conform to the 3-layers model and to a  $\Delta B^+$  defined uniquely by velocity should also conform to the drag reduction versus  $V$  scaling procedure.

Although several studies were published about the diameter effect of drag-reducing polymer solutions, we are only aware of a few covering drag-reducing surfactant solutions, e.g. [3,4]. Schmitt et al. [3] proposed a compound procedure where the drag reduction was plotted as a function of  $\tau_w$  (i.e. essentially the

same as drag reduction versus  $u^*$ ) for high  $\tau_w$ , and  $V$  as a function of  $\tau_w$  for lower  $\tau_w$ . This procedure fitted well the experimental data for their solution of C<sub>16</sub>TaSal surfactant. However, their procedure shows about 15% of systematic deviation in drag reduction when applied to experimental data for polymer solutions for which our drag reduction versus  $V$  procedure, on the other hand, provides close to a perfect fit [1]. This is a significant difference which could presumably suggest that polymer macromolecules and surfactant micelles interact with turbulence in different ways. Indeed, although at first sight most aspects of drag reduction (DR) by surfactant solutions seem to be the same as those of drag reduction by polymer solutions, there are, however, significant rheological and phenomenological differences [5,6]. For instance, it has been shown consistently that higher levels of drag reduction and HTR can be achieved by surfactant solutions than by polymer solutions. Also, measurements of the velocity profile in pipe flow of drag-reducing surfactant solutions apparently showed some departures, e.g. a noticeable ‘S’ shape, from Virk’s 3-layers velocity profile suggested for polymer solutions [6,7]. These differences raised questions about a possible fundamental difference in the drag reduction behavior of both types of solutions. On the other hand, Bewersdorff and Berman [8] suggested that the difference in the velocity profiles may be explained merely by the effect of changing viscosity, which may be much higher than the viscosity of the solvent in the case of surfactant solutions. This is a complex issue because it may not be easy to define meaningfully the solution shear viscosity in a turbulent flow field. Drag-reducing polymer solutions at the concentrations generally used, do not show at high shear rates a viscosity differing significantly from that of the solvent, however.

The significance of the use of proper shear viscosity for surfactant solutions is also stressed in another scaling procedure, proposed by Usui et al. [9]. This procedure is harder to test than the one proposed by Schmitt et al., because it relies on the use of a fluid relaxation time, or more precisely, on its dependence on the shear rate, which is diameter dependent. A previously published eddy diffusivity model by Usui et al. was used as a basis for this relatively complex numerical scaling procedure. In another recent paper on the diameter effect, Sood and Rhodes [4] propose a scaling procedure claimed to be of general validity for all drag-reducing solutions. Their numerical method assumes a damping factor applied to the Von Karman constant (usually assumed to be a constant value applicable to the whole Newtonian core region). This damping factor as well as the effective thickening of the viscous sublayer are determined from the experimental friction measurements on one single diameter test tube.

There is another phenomenological difference between polymers and surfactants that is seen in the region where mechanical degradation effects are present (the supercritical region). This is not directly related to different mechanisms of drag reduction, but rather to differences in the nature of the degradation process, which should be understood as a change of fluid properties. Degradation of polymer solutions is a process which develops on a relatively long time scale but is cumulative and permanent. This means that under steady flow conditions (i.e. constant wall shear rate) the fluid shows a permanent decrease in the drag reduction level due to the scission of large polymer molecules. This effect occurs mostly at singular points along the circulation system where shear and elongational stresses are highest (at the pipe entrance for example). On the other hand, in the case of pipe flow of surfactant solutions, the drag reduction for a given fluid is a fixed function of the wall shear rate, and the (reversible) degradation almost immediately reaches an equilibrium and no longer changes with time. This allows us to define a steady state drag reduction for surfactant solutions in the supercritical region, which is not possible for polymer solutions.

Note that the supercritical region, even for surfactant solutions, is controlled by physical processes that are very different than those influencing the subcritical one, and no single correlation is therefore likely to address satisfactorily the diameter effect in both regions. In this article we are focusing our attention on the subcritical region, where there is no degradation.

Given all these distinctions between polymers and surfactants, the question of whether or not the diameter effect scheme we proposed earlier for polymers could work equally well for surfactants is quite interesting. In addition, the diameter effect can be related to the broader issue of the comparison of polymeric and surfactant drag-reducing fluids, and, therefore, to the elucidation of the mechanisms responsible for the drag reduction phenomenon.

Another important context in which the diameter effect can be examined is the Type A/Type B distinction proposed for drag-reducing polymer solutions. The idea of two types of drag reduction has been discussed in detail by Virk and Wagger [10,11], and they have shown that a variation in NaCl concentration from  $10^{-2}$  to  $10^{-5}$  ppm may lead to a change from Type A to Type B behaviors. This difference was related to the conformation of the polymer molecules, which in turn seemed to vary dramatically depending on the concentration of ions in the solution (e.g. the amount of NaCl in the polyacrylamide solutions). The Type A drag reduction is typical for coiled polymer molecules (e.g. at high salt content), which require a certain level of wall shear stress before the onset of drag reduction takes place. As flow velocity increases further, so does the drag reduction, until degradation becomes apparent later on. This kind of polymer solutions exhibits a 3-layers velocity profile (referred hereafter as '3L' fluids), and their diameter effect is correlated well by our scaling procedure drag reduction versus  $V$ . This was the case, for instance, for polyacrylamide, polyox, and guar gum solutions [1]. On the other hand, Type B drag reduction is typical of extended polymer molecules (e.g. polyacrylamide solutions with very low salt content), which exhibit asymptotic drag reduction immediately after transition from laminar to turbulent flow. With increasing flow velocity, the asymptotic friction coefficients are maintained until a retro-onset point is reached, after which the drag reduction level remains approximately constant for a given pipe diameter with the further increase of velocity. If this is correct, for Type B drag reduction a true diameter effect could only be seen in the region after the drag reduction departs from the maximum drag reduction asymptote (MDRA) and before degradation takes place.

## 2. Experimental setup and procedure

Details of the experimental setup used for the friction coefficient measurements have been described in previous articles (e.g. [12]). It consists basically of a set of five pipes of different diameters (2, 5, 10, 20, and 52 mm). All of them can be supplied with fluid by either variable speed pumps or pressurized tanks. This setup allows us to obtain a wide range of mean flow velocities (up to about  $20 \text{ m s}^{-1}$ ). Since the tests for the supercritical region require higher mean velocities, and, therefore, larger available pressures, a few modifications were done to the existing setup, such as providing smaller pressurized vessels (which can stand higher pressures) to drive the fluid through the pipes of smallest diameters. In this case, little fluid is required, but high pressures are needed to obtain the high flow velocities. On the other hand, reaching steady state with weak surfactant solutions may require a long pipe, especially at low velocities in large pipes, i.e. at low shear stress. This is due to the long induction time needed for the formation of the shear-induced state (SIS), a superstructure of micelles induced by the shear. Note that in this case we are dealing with the simultaneous development of fluid properties and flow field. Of course, both processes may be present as well in the flow of polymer solutions, but in this latter case (and likely for strong surfactant solutions also), the time scale characteristic of fluid change due to flow is probably negligible compared with the time scale for flow development. For polymer solutions (which were used in most entry lengths studies found in the literature), the development of the flow takes place over entry lengths

fairly well quantified by a known  $L/D$  (say, 200 for momentum and 1000 for heat), whereas the pipe lengths needed for SIS formation may be considerably longer. Therefore, pipes of length and diameter similar to those of the test pipes were installed upstream of the test section, and the friction coefficients were also measured in that region to ensure fully-developed flow.

As in the tests with polymer solutions, the pressure drop measurements were taken by differential pressure transducers over the section of pipe where flow is already fully developed. Temperature was always monitored, to ensure that the diameter effect tests were as close to isothermal conditions as possible. Altogether, the experimental error in drag reduction is expected to be within 1–2% for the four smallest pipes, and between 2 and 3% for the biggest (details of error estimates can be found elsewhere [1]).

To resolve some uncertainties, we made use of local measurements of turbulent exchange mechanisms across the pipe cross section in addition to the classic integral measurements of friction coefficient. However, rather than measuring velocity profiles, we measured temperature profiles, for reasons explained hereafter. For this purpose we developed a temperature sensor made from 0.003 in. E-type thermocouple wire, and which can be moved across the pipe cross section. The full description of this setup can be found elsewhere [13]. Besides temperature profile measurements for each run, we also measured the overall heat transfer coefficient at the same location. The agreement between Nusselt number calculated from the overall heat transfer measurements and Nusselt number calculated from the temperature profile measurements was within 10%. Drag reduction was measured as well during the heat transfer measurements.

As our objective was to study the large differences in the level of drag reduction in different tubes at a given Reynolds number, strong drag-reducing solutions (e.g. high concentrations) are obviously a poor choice, because they would show asymptotic drag reduction in all tubes. Solutions with lower concentrations are good from this point of view, but their structures break more easily at higher velocities (Reynolds numbers), thus limiting the subcritical range. The two requirements, lower drag-reducing effectiveness and higher critical stress, are, unfortunately, generally mutually exclusive. A proper compromise must therefore be found in choosing the best concentration for a given fluid. Those two fluid properties, and their relationship, depend on the chemistry of the fluid, however, and during our experimenting with surfactant solutions, we noticed that the fluid's drag-reducing properties were changing with time. Chemical agents (most noticeably copper hydroxide,  $\text{Cu}(\text{OH})_2$  originating from copper or brass parts in the circulation loops) caused a phenomenon which we refer to as 'stiffening' [12]. In general, a stiffened fluid is able to stand higher shear stresses, whereas it shows less drag reduction at lower Reynolds numbers. Such a stiffened surfactant solution is therefore a good choice for the study of the diameter effect. Not only does it have higher critical shear stress and shows less drag reduction at lower Reynolds numbers, but it is also more chemically stable than the 'unconditioned' fluid at the same concentration. An additional benefit of the conditioned fluid is that its viscosity is practically the same of water, which simplifies the interpretation of results.

It was decided therefore to prepare the fluid for the diameter effect tests by adding 3.75 mM of  $\text{Cu}(\text{OH})_2$  to a solution of 2000 ppm of fresh active surfactant (from an Ethoquad T13-27 master solution by AKZO Chemicals) mixed with 1740 ppm of sodium salicylate (NaSal) as counterion (a counterion to surfactant molar ratio of 2.5), all in tap water. Ethoquad T13 is a tris (2-hydroxy-ethyl) tallowalkyl ammonium acetate [(tallowalkyl- $N$ -( $\text{C}_2\text{H}_4$ )OH) $_3$  Ac]. (In this article, when quoting concentrations we refer to the fraction of actual surfactant in the test solution we prepared, not including solvent already present in the master solution as received from the manufacturer.)

In the course of our experiments we realized that some other surfactant had to be used besides the Ethoquad because of the non-suitability of the scaling procedure reported by Schmitt et al. [3] for the Ethoquad data. Accordingly, we also used a 4000 ppm nonionic surfactant solution in tap water. This biodegradable surfactant, SPE95285, was kindly developed for our experiments by Dr. M. Hellsten of AKZO-Nobel Chemicals. It is a mixture of two nonionic surfactants. One consists of ethoxylated unsaturated fatty alcohols (mainly oleyl alcohol) and the other of ethoxylated unsaturated fatty acid ethanalamides, where the main component of the fatty acids is oleic acid. The chemical structure of these two components is  $R(\text{OCH}_2\text{CH}_2)_m\text{OH}$  and  $R_1\text{CONH}(\text{CH}_2\text{CH}_2\text{O})_n\text{H}$ , respectively, where  $R$  and  $R_1$  stand for the unsaturated alkyl chains and  $m$  and  $n$  represent the mean number of ethylene oxide groups in the hydrophilic chains [22]. This surfactant was developed to operate effectively in the 5–25°C range, but still showed drag reduction ability up to 40°C at concentrations of about 4000 ppm. Besides its nonionic nature, this surfactant has very different properties than those of Ethoquad. In the nonionic case, a reduction of viscosity relative to water and an eventual loss of drag-reducing ability at increased temperatures is seen, and is due to phase separation (solubility problem). Transition from cylindrical to globular micelles appears at low temperatures. Both are the opposite of what happens with Ethoquad solutions. This nonionic surfactant was chemically stable, but an initial concentration of about 500 ppm of biocide (Nalco 2810) had to be added to prevent biodegradation. The surfactant shear viscosity was more than twice as high as that of water at room temperature for the relevant shear rates, however. As mentioned above, the interpretation of the results is easier if the fluid viscosity is kept as close to water as possible, and the viscosity of this solution was therefore controlled by conducting the tests at higher temperatures (around 34°C), where this fluid shows water-like viscosity due to surfactant precipitation, but yet exhibits high levels of drag reduction [13].

Somewhat lower concentrations of the same types of surfactants were prepared to measure temperature profiles, namely a 1500 ppm Ethoquad solution with a 2.5 M ratio of NaSal counterion to surfactant diluted in tap water, but without the  $\text{Cu}(\text{OH})_2$ ; and also a 2000 ppm of SPE 95285 nonionic surfactant solution with a small amount of biocide (100 ppm of Nalco 2810), also diluted in tap water.

Finally, two types of polymer solutions were also used: (1) two intentionally degraded solutions (500 and 1500 ppm) of polyacrylamide (Separan AP-273 by Dow Chemicals) diluted in deionized (DI) water. These highly concentrated solutions were continuously circulated around a short loop with a partially throttled valve, until constant shear rate capillary viscosity measurements at  $1000 \text{ s}^{-1}$  showed a decrease in the viscosity of both solutions from about 15 and 20 cP, respectively, to 5 and 8 cP. (2) a 150 ppm polysaccharide (Xanthan gum by Kelco) solution in deionized water. The latter polymer solution was used to study Types A and B characteristics in light of the scaling procedures. Unfortunately, for both kind of polymer solutions, it was not possible to obtain water-like viscosities, even at the high wall shear stresses that were expected in the actual diameter effect experiments. Therefore, a reasonable way to calculate the solution friction coefficients was by the use of the ‘apparent’ viscosity at the wall, which is the viscosity measured under laminar flow at the same wall shear stress expected in the actual turbulent test. For this purpose we used a capillary viscometer with tube diameters ranging from 0.178 to 2 mm in order to cover the range of shear rates present in turbulent flow, as described in detail in [12].

Evidently, there are many more drag-reducing fluids available. However, as we have shown before [1], most of the well-known fluids usually are of the 3L-type, and therefore should scale according to the drag reduction versus  $V$  correlation. One of our objectives was to see if fluids which do not follow this pattern might be classified according to different types of scaling and turbulent profiles.

### 3. Results

#### 3.1. Integral measurements of friction

Fig. 1 shows results of the drag reduction tests with the Xanthan gum, a well known Type B drag-reducer. Although Rochefort and Middleman [14] showed that this polymer exhibits Type B drag reduction even at a very high salt content, we prepared our solution with deionized water. As can be seen, for pipe diameters of 10, 5, and 2 mm, there is typical Type B behavior, i.e. an asymptotic drag reduction starting from the laminar-turbulent transition region. At a Reynolds number of about 10,000, however, the  $C_F$  versus  $Re$  curves for the smaller pipe diameters depart from the asymptote, in most cases ending up approximately parallel to the Prandtl–Karman curve for Newtonian turbulent flow (this translates to a constant value of drag reduction) before degradation. (Of course, eventually, at a large enough shear stress, the fluid will begin to experience permanent mechanical degradation, as is seen shortly after the departure from the asymptote for the 2 mm pipe and later for the 5 mm pipe.) The two larger pipes (20 and 52 mm) show, however, more typical Type A behavior. (Liaw et al. [21] in a study of the effect of molecular characteristics of polymers on drag reduction, observed a similar effect of pipe diameter for polyethylene oxide in Benzene.) This suggests that Types A and B drag reduction s may be the expressions of two regions of drag reduction process that can be encountered for a given fluid in a given pipe. In pipes of smaller diameters, the flow intensity (shear stress) at a given Reynolds number may be large enough to stretch the molecules of the fluid enough to provide asymptotic drag reduction immediately after the

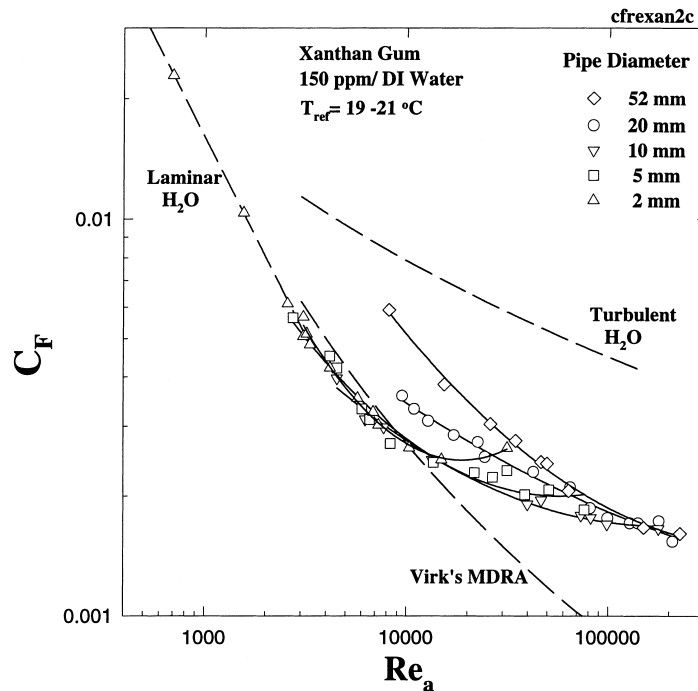


Fig. 1. Friction coefficient for five pipe diameters (52, 20, 10, 5 and 2 mm) as a function of apparent Reynolds number for a 150 ppm Xanthan gum solution in DI water. Virk's MDRA for polymers is shown for reference.

laminar-turbulent transition region. (Of course, this is more likely for a solution with molecules already more extended under static conditions.) On the other hand, for pipes with very large diameters, even molecules already very stretched under static conditions may need shear beyond the laminar-turbulent transition region to show drag reduction effects. Looking at one given pipe diameter exhibiting Type A behavior, say the 52 mm diameter pipe, the drag reduction process consist of Type A-like behavior (i.e. onset from Newtonian friction and strong diameter effect) at low velocities, followed by Type B-like behavior (i.e. constant drag reduction level as extended from asymptotic value at retro-onset) at high velocities. We do not have additional data to confirm this conclusively, but Fig. 1 also strongly suggests that the friction curves for all diameters merge into one master curve. (A similar convergence may also be present in Liaw et al. [21] data for 0.05% WSR in benzene.) Furthermore, this master curve appears approximately parallel to the Newtonian curve at high Reynolds numbers. (Some indications of such a feature may also perhaps be extrapolated from data shown in Ollis [23].)

Of course, this effect can only be seen clearly if there is little or no degradation taking place, which is why we used a Xanthan gum solution which exhibits a high resistance to mechanical degradation. This was verified by repeating some runs with a fluid sample that had already passed through a given pipe, and testing it again at about the same shear stress conditions (ranging from 1200 to 50,000 N m<sup>-2</sup>). For tests carried out in the region where the  $C_F$  curves depart from the MDRA, but remains approximately parallel to the Newtonian curve, we only found differences in the  $C_F$  measurements between successive runs that fall within the experimental uncertainty. (Of course, at high enough shear rate, mechanical degradation will indeed eventually take place as seen for the 2 mm pipe and perhaps the 5 mm one.) This suggests that the departure from the MDRA at higher Reynolds numbers is not related to a mechanical degradation, and suggests instead that the drag-reducing effectiveness of the fluid has reached a maximum. This is contrary to prevalent belief among many drag reduction researchers, who sometimes automatically associate the apparent ‘loss’ of drag reduction after retro-onset to fluid degradation, be it mechanical, chemical, biological, etc.

If we add stretching of the molecules to our interpretation of the interactions between flow and polymer molecules, this would mean that polymer molecules are ‘fully’ stretched after the retro-onset, and, therefore, that a further increase in the frequency of the turbulence dynamics cannot be followed by changes in the polymer molecules. Other interpretations are possible, of course. Excluding the signs of degradation for the 2 mm and maybe 5 mm pipes, we can see from Fig. 1 that the friction curves for all pipe diameters exhibiting Type B at low velocities converge to the same line, approximately parallel to the Prandtl–Karman curve, and thus exhibit a roughly constant drag reduction. Therefore, this already suggests that the diameter effect is not significant for pipes showing an initial Type B behavior, in this case those with diameters equal or less than 10 mm, assuming no mechanical degradation. Furthermore, for the 20 and 52 mm pipes, those showing Type A behavior at low velocities, the diameter effect apparently exists only in the region where molecules are likely still affected by the flow, i.e. before they merge with the other curves and become then more Type B-like themselves.

Altogether, all the friction curves, whether they correspond to Type A or B at low velocities, suggest that the diameter effect disappears at high Reynolds numbers if no degradation is involved, and also that the drag reduction level becomes thereafter a parameter approximately independent of Reynolds number. If this observation is of general validity, it would constitute a very interesting development towards a better fundamental understanding of the drag reduction phenomenon, in that a much stronger and simpler correspondence to Newtonian flow could be made in that region. Further work should be conducted to verify this hypothesis.

Some extension of the Type A/Type B relationship may hold for surfactant solutions as well. Both Types A and B behaviors are also observed for surfactant solutions. However, in the case of surfactant solutions the flow affects primarily the formation of the SIS rather than of the micelles themselves. Mechanical degradation is also harder to avoid, although it is only temporary.

Note that data in Fig. 1 lie below Virk's asymptote at low  $Re$ . Indeed, it is now believed that asymptotic polymer solutions can give drag reduction greater than that predicted by Virk's earlier MDRA, and also that the latter may be underestimating even more asymptotic drag reduction for *surfactant* solutions. Zakin et al. [15], for example, showed a lower asymptote for surfactants based on their compilation of data from different authors; and a recent correlation we developed for asymptotic drag reduction for surfactant solutions [13] shows even somewhat higher level of drag reduction in the region of low Reynolds number than that proposed by Zakin et al.; and therefore much higher than Virk's.

In Fig. 2, the friction coefficients for a conditioned Ethoquad solution are plotted as a function of Reynolds number. A strong diameter effect is seen in both subcritical and supercritical regions. An envelope of minimal  $C_F$  is approximately parallel to the curve for turbulent flow of Newtonian fluids (i.e. showing constant drag reduction). This could again mean that there is a maximum achievable drag

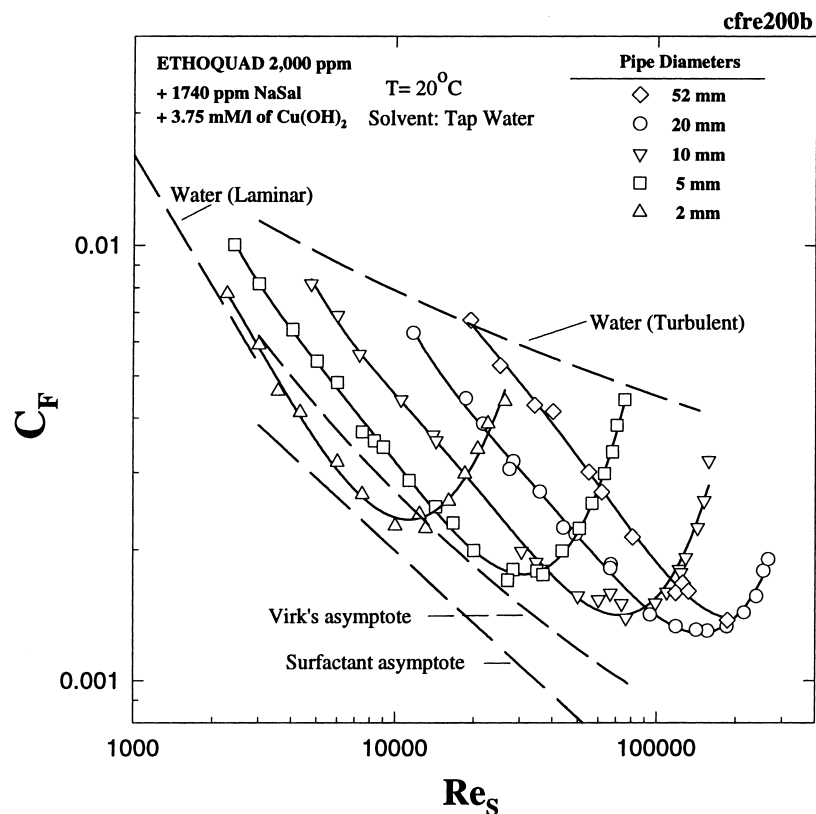


Fig. 2. Friction coefficient for five pipe diameters (52, 20, 10, 5 and 2 mm) as a function of solvent Reynolds number for a 2000 ppm Ethoquad T13/27 solution in tap water plus 1740 ppm of NaSal and  $3.75 \text{ mM l}^{-1}$  of  $\text{Cu}(\text{OH})_2$ . The MDRA for polymers (Virk) and surfactants (Zakin et al.) are plotted for reference.

reduction level for this fluid that is independent on pipe diameter, but conceivably the temporary degradation effects seen for surfactant solutions could have affected the shape of this envelope.

Note that this fluid exhibits a shear viscosity very close to that of water and that the diameter effect shown here is therefore indeed a true one, unlike some apparent diameter effects that are merely a result of the use of an inadequate viscosity (the solvent viscosity for example) in the Reynolds number, as we showed in earlier work. Although the data in Fig. 2 does not extend to the onset region for all pipes, it is nevertheless possible to extrapolate the curves and to estimate the onset shear stress for each pipe. If we do so, we find onset shear stresses of 1.06, 0.45, 1.0, and 0.446  $\text{N m}^{-2}$  for the 5, 10, 20, and 52 mm pipes, respectively. This suggests that the onset shear stress is also relatively independent of diameter, as is believed to be the case for polymer solutions.

Fig. 3 shows the same data as that of Fig. 2, but plotted according to the scaling procedure we proposed for polymer solutions, i.e. drag reduction versus  $V$ . Up to about  $6 \text{ m s}^{-1}$ , i.e. in the subcritical region where no apparent signs of degradation are noticeable, all data seem to be very well correlated by a single curve. It can also be seen that even the very small diameter (2 mm) pipe, which could not be satisfactorily included by some other procedures, is well correlated with this approach. Over the range of increasing drag reduction the variations in drag reduction for the various diameters are not more than 5–7% at a given velocity. More importantly, the deviations are randomly distributed, suggesting that they are not directly related to pipe size issues, but are instead likely attributable to random uncertainties in the experimental procedure. The correlation seems very good given the simplicity of the scaling procedure, and is in fact better than the fit of the more complicated procedures proposed earlier.

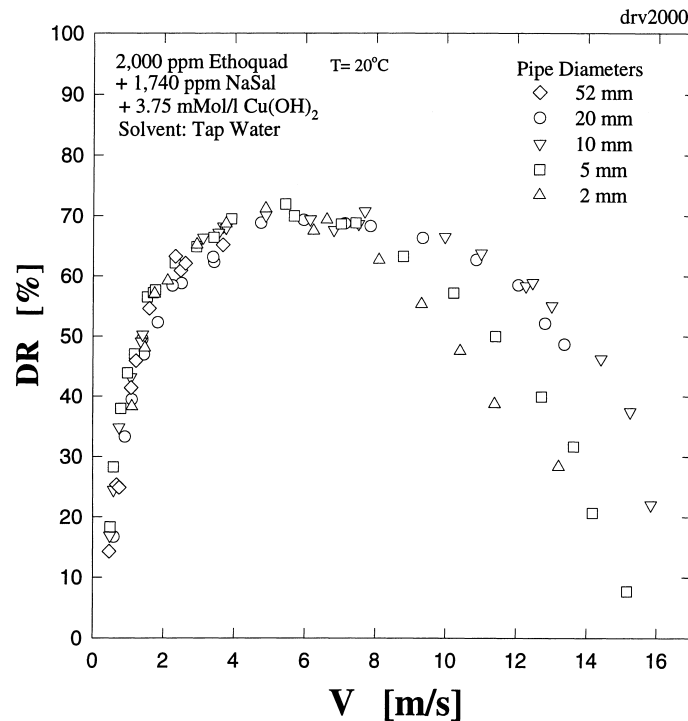


Fig. 3. Drag reduction level as a function of bulk velocity ( $V$ ) for the data shown in Fig. 2.

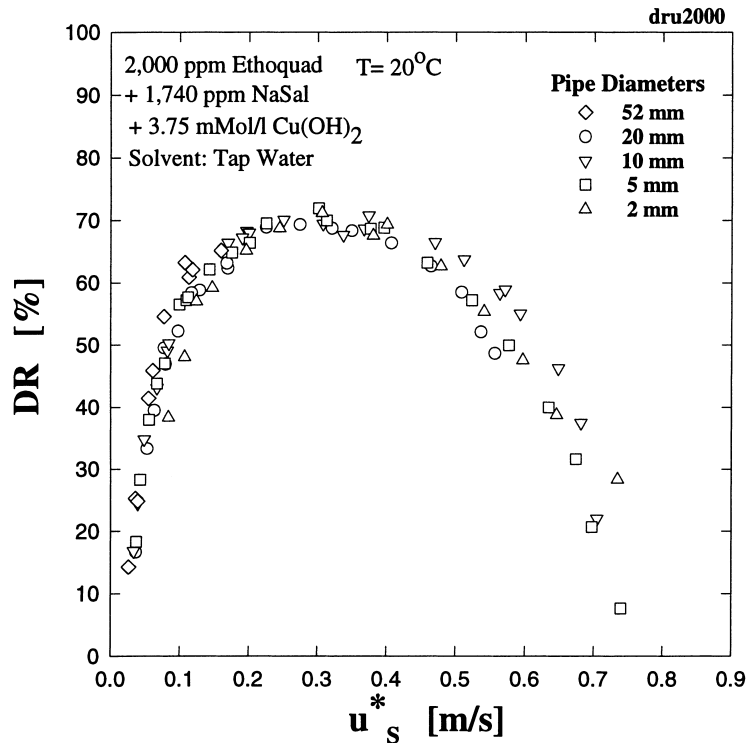


Fig. 4. Drag reduction level as a function of solvent shear velocity ( $u_s^*$ ) for the data shown in Fig. 2.

In the supercritical region, the dominant process is the fluid's degradation [16], which is of different nature for surfactant and for polymer solutions. For the polymer solutions, it is a cumulative effect which leads to a continuous change in the fluid properties due to permanent degradation, whereas for the surfactant solutions, the change in the fluid properties is only temporary. It is generally believed from previous work that the temporary degradation of surfactant solutions begins at a critical shear stress approximately independent of pipe diameter. This can indeed be seen in Fig. 4, where drag reduction is plotted versus shear velocity ( $u^*$ ), as taking place for a  $u^*$  of about  $0.3 \text{ m s}^{-1}$ . It is therefore not surprising that in the supercritical region the shear stress (or shear velocity) is a better parameter for predicting the level of drag reduction for a given fluid than is the velocity. The difference between Figs. 3 and 4 does not appear large in the subcritical region because of the scale used for the figures, but the drag reduction/ $V$  approach does indeed lead to a significantly better correlation of all the diameters in that region. Perhaps more importantly, it is also much more meaningful physically. The reader is referred elsewhere for a more elaborate discussion of this issue [1].

We also tested with our Ethoquad data the  $\tau_w$  versus  $V$  procedure which Schmitt et al. applied successfully to a  $C_{16}\text{TaSal}$  surfactant solution. As can be seen in Fig. 5, at a given flow velocity, the wall shear stresses between the 2 and 52 mm tube differ by a factor of about 2 for a given velocity, which is a large difference compared with the good fit achieved by Schmitt et al. for their surfactant solution ( $C_{16}\text{TaSal}$ ). Apparently, these two surfactant solutions scale best in two completely different representations: the Ethoquad surfactant scales exceptionally well using the same correlation as most polymer

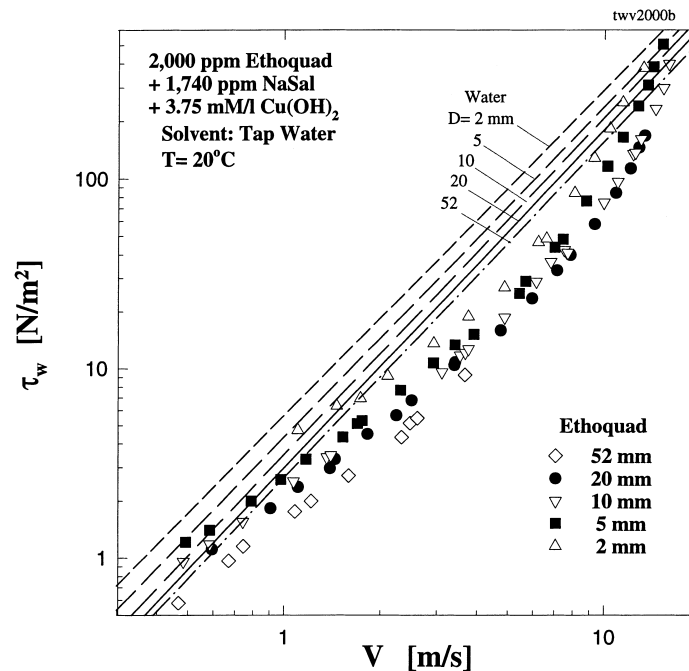


Fig. 5. Wall shear stress for five pipe diameters (52, 20, 10, 5 and 2 mm) as a function of bulk velocity for the data shown in Fig. 2. The straight lines are the theoretical values for water.

solutions, i.e. drag reduction versus  $V$ , whereas the  $C_{16}TaSal$  surfactant scales best according to the  $\tau_w$  versus  $V$  correlation.

Our earlier analyses of the drag reduction versus  $V$  scaling procedure for polymer solutions showed that any given solution which conforms to the 3-layers model in conjunction with the displacement of the elastic sublayer ( $\Delta B^+$ ) being function of  $V$  rather than  $u^*$ , should satisfy a fixed relationship between drag reduction and  $V$  that is independent of the tube diameter (and better correlated than the corresponding drag reduction versus  $u^*$  [1]). The Ethoquad surfactant is therefore likely to have a velocity profile similar to the 3-layers model for polymers, whereas the surfactant used by Schmitt et al. is not.

To attempt to resolve this issue, we decided to test another surfactant. This is a nonionic surfactant (SPE 95285) with very different properties than Ethoquad's. Its phase diagram is a 'mirror' image of that for Ethoquad in that phase separation takes place at higher temperatures for a given concentration of the nonionic solution, and transition from cylindrical to globular micelles takes place at low temperatures.

In addition, we also decided to test polymer solutions with characteristics rather different from those of commonly used solutions, e.g. in our case high concentrations of low molecular weight polymer rather than the usual dilute solutions of high molecular weight polymers. To achieve this, we prepared high concentrations of Separan solutions (500 and 1500 ppm), the molecular weight of which was intentionally reduced by mechanically degrading the fluids through circulation for several hours through a partially-closed control valve. These degraded high-concentration fluids provided a level of drag reduction comparable with that of solutions with 20 or 30 times lower concentrations of very high molecular weight polymers.

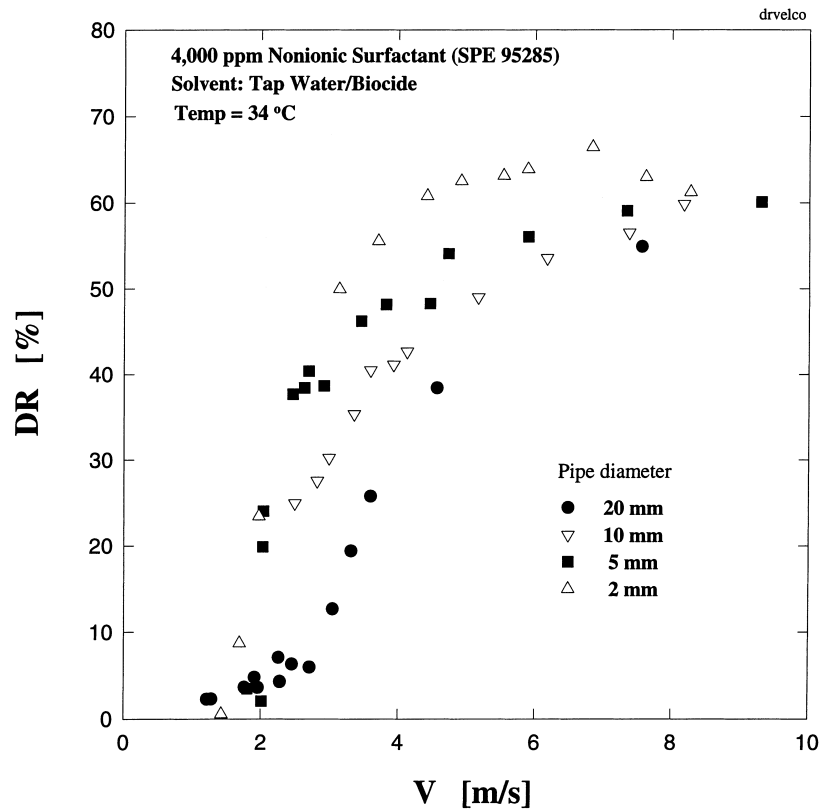


Fig. 6. Drag reduction level as a function of bulk velocity ( $V$ ) for a 4000 ppm SPE 95285 (nonionic surfactant solution) in tap water plus an initial 500 ppm of biocide. Note how this representation fails to correlate the diameter effect by as much as 30% between the 2 and 20 mm diameter pipes, and how smaller diameter pipes show larger drag reduction than bigger ones.

Results for the nonionic surfactant are presented in Figs. 6 and 7. Scaling drag reduction with velocity (Fig. 6) obviously does not work satisfactorily, as seen when compared with Fig. 3 for Ethoquad. For a given velocity, there is up to 30% more drag reduction in the 2 mm tube than in the 20 mm tube. The data for the other two tube diameters lie in between. On the other hand, Fig. 7 shows the data for all four diameters well correlated by a straight line when the data are plotted as  $\tau_w$  versus  $V$  (except for a few data around the onset points, and for some showing signs of degradation in the 2 and 5 mm tubes at high velocities). This surfactant solution shows therefore the same diameter scaling pattern as that tested by Schmitt et al.

The situation with the partially degraded high concentration polymer solutions shows an intermediate behavior. Fig. 8 shows that our proposed scaling correlation, drag reduction versus  $V$ , does not work as adequately for these fluids (especially for the 1500 ppm Separan solution as shown by the solid line) as it does for the Ethoquad solution seen in Fig. 3, or for the other polymer solutions reported on in Gasljevic et al. [1]. Similarly, the alternative approach,  $\tau_w$  versus  $V$ , as shown in Fig. 9 does not correlate well the data for all diameter pipes in one single curve, as it did on the other hand for the nonionic surfactant seen in Fig. 7. Apparently then, the two scaling correlations discussed above may well represent two limiting cases, and although the diameter effect problem for a large variety of fluids may be taken successfully

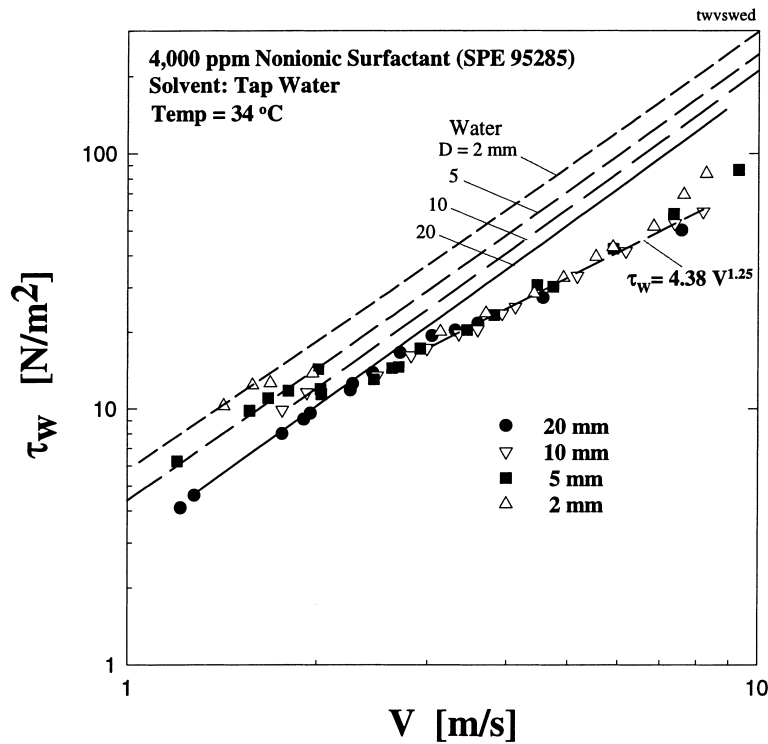


Fig. 7. Wall shear stress as a function of bulk velocity for the data shown in Fig. 6. The straight lines are the theoretical values for water. This representation provides a good scaling procedure for this particular fluid. The solid line through the data shows a best-fit power-law correlation in the intermediate non-degraded regime.

predicted using one of these correlations, some other fluids may indeed show intermediate behaviors that would not be well represented by either one of these correlations.

To summarize, we have distinguished two types of representations correlating the diameter scaling for drag-reducing solutions: drag reduction versus  $V$ , and  $\tau_w$  versus  $V$ ; and drag-reducing solutions which scale well in one representation do not scale well in the other. It appears that those solutions which scale well in the  $\tau_w$  versus  $V$  representation show a stronger diameter effect than those which scale well in the drag reduction versus  $V$  representation. Indeed, when plotted in drag reduction versus  $V$  presentation, the fluids that scale well with  $\tau_w$  versus  $V$ , still show a higher drag reduction in smaller pipes than in bigger ones at the same  $V$ . In addition, as the 500 and 1500 ppm Separan solution suggest, some other fluids may show an intermediate behavior between these two extremes.

Also, our measurements suggest that Types A and B drag reduction are more likely pertaining to two different regions of the same process rather than to two distinct types of fluids or of drag reduction phenomena. As mentioned above, in the case of Type B fluids, polymer molecules may be 'stretched' fully after the retro-onset, and, therefore, a further increase in frequency of the turbulence dynamics could not result readily in changes in molecular configuration. The diameter effect also appears to disappear in that region. A more detailed analysis of the Type A versus Type B behaviors will be presented shortly in another article. Again, it is worth noting also that the distinction between the two scaling behaviors identified here is not simply one between polymer and surfactant solutions as one might perhaps have expected.

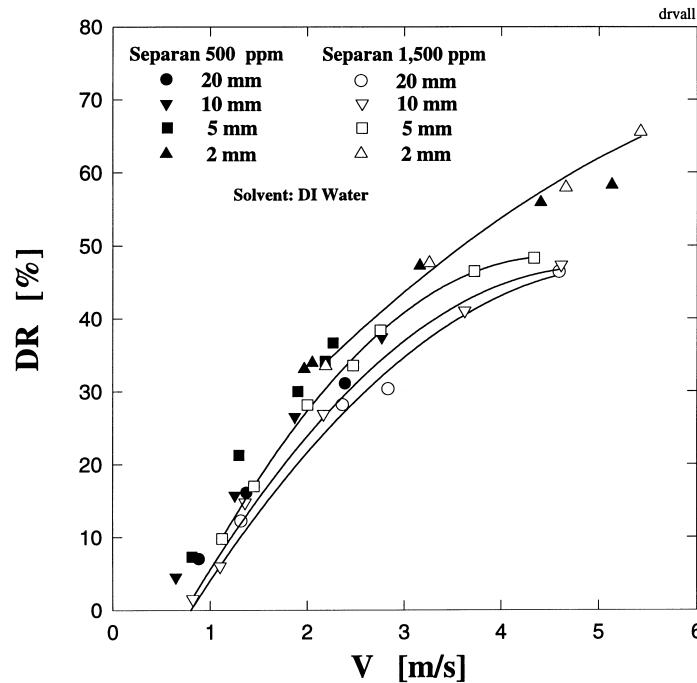


Fig. 8. Drag reduction as a function of bulk velocity for two mechanically degraded Separan solutions (500 and 1500 ppm). Curve fits for the 1500 ppm solution data are shown by the solid lines. Note the larger spread between data than in Fig. 3 before degradation.

### 3.2. Local measurements-temperature profiles

The two different scaling procedures suggest distinct interactions between the flow and the drag-reducing agent in the velocity regime where the solution properties (such as shear viscosity and elasticity) are affected by the flow. Some departure from optimal scaling may be attributed to the effects of a shear-dependent viscosity, which for some drag-reducing fluids (especially surfactant solutions) may indeed sometimes be significant. However, as mentioned before, we have taken steps to minimize these effects, and we have used fluids with water-like viscosities for the purpose of clearly showing the distinction between the two procedures. To understand better the nature of the fluid/flow interaction, one can also make use of local measurements such as the velocity or temperature profiles, rather than integral measurements like the friction or heat transfer coefficients.

Velocity profile measurements for Separan and other polymer solutions that conform to the drag reduction versus  $V$  scaling procedure have been published earlier. Those velocity profiles are in good agreement with Virk's 3-layers velocity profile, and as our analyses suggest [1], there is a correlation between the 3-layers velocity profile and the proposed drag reduction versus  $V$  scaling procedure. (We call hereafter fluids of this kind '3L' fluids.) Instead of measuring velocity profiles, however, we decided to measure temperature profiles for the fluids we used in our study of the diameter effect. We have indeed recently developed a technique for measuring the temperature profiles of drag-reducing fluids in the context of a study of the turbulent Prandtl number ( $Pr_t$ ). For asymptotic fluids (for which velocity profiles are well

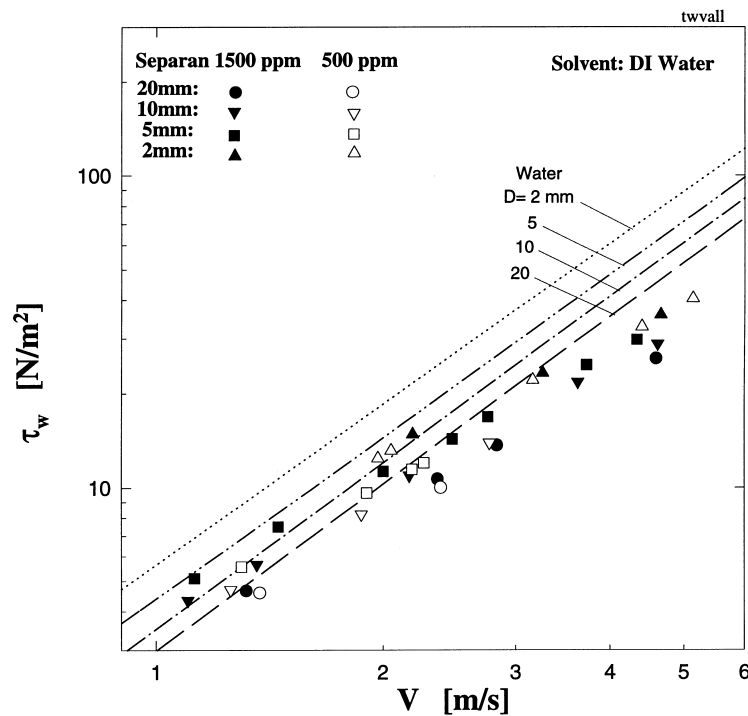


Fig. 9. Wall shear stress as a function of bulk velocity for the data shown in Fig. 8. The dashed lines are the theoretical values for water. Note the larger spread between data than in the intermediate region of Fig. 7.

known both for some polymers and surfactants), we measured various temperature profiles, and, came to the conclusion that the  $Pr_t$  is about constant across the pipe, with a numerical value of 5–8 depending on the fluid [13]. This implies a good analogy between the velocity and temperature profiles, allowing us therefore to use measurements of the temperature profile instead of velocity profiles for the analysis of drag-reducing flows. As our technique for temperature measurements is also fast and accurate, it was more convenient to use temperature profile measurements considering the large number of measurements needed. In addition, our measurements showed that for all fluids tested, the diameter effect on drag reduction was analogous to the diameter effect on heat transfer reduction [17], another indication of strong correlation between the momentum and heat transfers.

In the present article we show only results of two typical temperature profile measurements pertaining to the surfactant solutions discussed above (others will be published elsewhere). Fig. 10 shows temperature profiles for an older 1500 ppm Ethoquad solution with a 2.5 M ratio of NaSal to surfactant, a fluid which showed excellent agreement with the drag reduction versus  $V$  scaling procedure. Temperature profiles were measured at various bulk flow velocities. As expected, the temperature profiles are analogous to the velocity profiles in Virk's 3-layers model: the elastic layer appears to grow with increasing bulk velocity, and the slope of the temperature profile in the elastic layer remaining approximately constant. Not surprisingly, the slope of the temperature elastic layer for this surfactant solution is about twice as large as that of the elastic layer in the temperature profiles of other 3L-type polymers [13]. For example, the elastic layer for the asymptotic profiles of polyacrylamide solutions is given by  $T^+ = (75 \pm 10) \ln(y^+) + \text{constant}$ ,

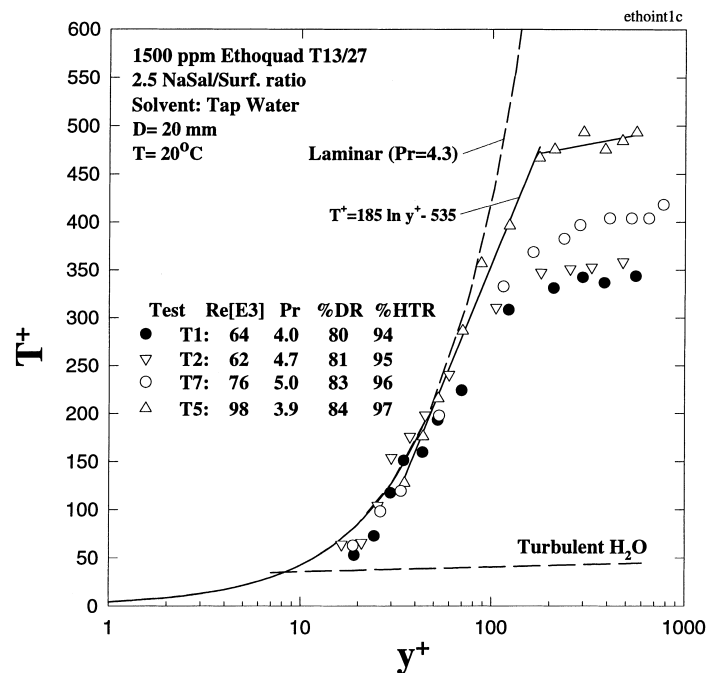


Fig. 10. Dimensionless temperature profiles for a 1500 ppm Ethoquad solution. Each profile was measured at a different Reynolds number (i.e. bulk velocity). ID = 20 mm.  $T_{\text{avg}} = 20^\circ\text{C}$ . Note how the profiles vary in a fashion similar to that of 3-layers velocity profiles. The solid lines are best fit linear regressions for profile T5 and correspond to asymptotic heat transfer (and drag) reduction conditions.

whereas for these asymptotic profiles of Ethoquad it is given by  $T^+ = (185 \pm 10) \ln(y^+) + \text{constant}$ . Similarly, it is also believed that the elastic layer in the velocity profile of some surfactant systems is about twice as steep as the velocity elastic layer for most polymers, consistent with the larger maximum drag and heat transfer reduction asymptotes observed for surfactants compared with polymers [18]. (Virk's asymptotic profile for polymers is given by  $u^+ = 11.7 \ln(y^+) + \text{constant}$ , whereas Zakin et al. proposed an asymptotic profile for surfactants given by  $u^+ = 22.4 \ln(y^+) + \text{constant}$ .) Measurements of drag reduction conducted simultaneously with each of these profiles indicated that at the highest Reynolds number measured (about 98,000), we had asymptotic drag reduction (according to the Zakin et al. [15] MDRA correlation). The corresponding temperature profile is seen in Fig. 10 with upright triangles (run T5), a best fit curve for this profile being shown in Fig. 10 as a solid line. However, as can be seen, a relatively large Newtonian core region remains towards the pipe center, unlike in the 3L model. This has also been observed for the velocity profile measurements of surfactant solutions which are presumably asymptotic as well [6,19]. We have recently shown, however, that upon the addition of small amounts of contaminants (such as copper hydroxide to Ethoquad solutions or sodium salicylate to nonionic surfactant solutions), a larger (e.g. 13% higher) elastic-layer slope may be seen, perhaps due to water-like viscosity in this case. Also, the Newtonian core seen in profile T5 of Fig. 10 disappears then, at least at low Reynolds numbers, with the elastic layer extending to the centerline, leading to an even lower friction coefficient, which means an even larger maximum drag reduction than that corresponding to the asymptote proposed by Zakin et al. These results will be shown in detail elsewhere.

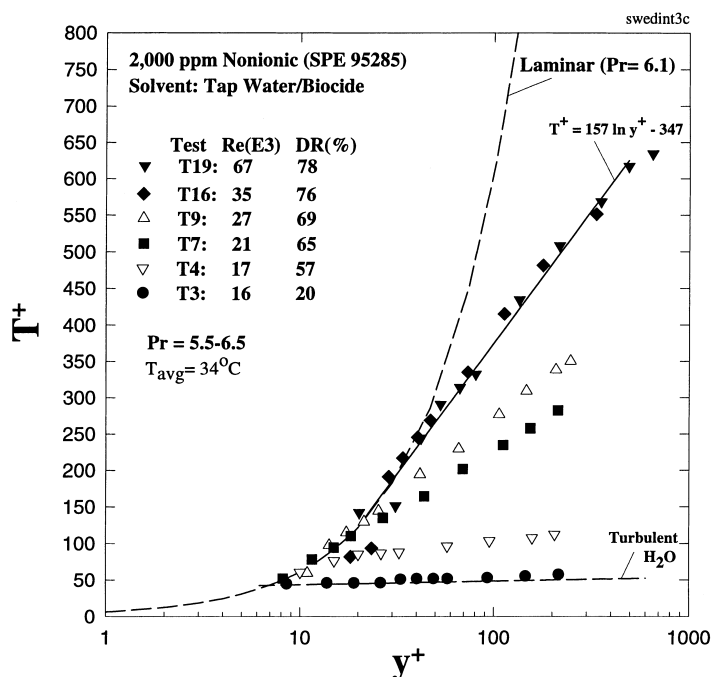


Fig. 11. Temperature profiles for a 2000 ppm SPE 95285 nonionic surfactant solution.  $T_{avg} = 34^{\circ}\text{C}$ . Each profile was measured at a different Reynolds number. Note how the profiles vary in a fan-type fashion. The solid line through the data is a best-fit linear regression for profile T19.

Fig. 11 shows temperature profile measurements for the nonionic surfactant SPE 95285, which conforms very well to the  $\tau_w$  versus  $V$  scaling procedure. We can see that there are no distinct elastic and core regions, and that the whole cross-section is affected by the drag-reducing effects, even at reduced levels of heat transfer. With larger flow velocity, the level of heat transfer reduction is increased by a steepening of the slope of the temperature profile rather than by growth of the elastic layer. In this case we can talk of a fan-type evolution of the temperature profiles (or velocity profiles) with the slope changing with increasing flow velocity and extending practically all the way to the center of the pipe; instead of the elastic layer growing in thickness with a constant slope, as was the case with Ethoquad. Bewersdorff and Ohlendorf [6] measured velocity profiles for the same  $C_{16}\text{TaSal}$  solution for which Schmitt et al. showed good agreement with the  $\tau_w$  versus  $V$  scaling procedure, and not surprisingly, the velocity profiles showed a fan-type development with increasing flow velocity, confirming a likely relationship between the fan-type profiles and the  $\tau_w$  versus  $V$  correlation. As in the case of the profile measurements for the Ethoquad solution, the drag reduction measurement for our nonionic surfactant solution corresponding to the profile measured at  $Re = 67,000$  (T19) is in reasonably good agreement with the MDRA proposed by Zakin et al. However, the addition of small amounts of NaSal enhanced the drag reduction (and heat transfer reduction) effectiveness of the fluid by about the same amount (10% in  $C_F$ ) as the  $\text{Cu}(\text{OH})_2$  did for the Ethoquad solution [13], possibly because of lower viscosity.

We can then summarize the difference between the two groups of drag-reducing fluids as follows: in one case (e.g. a solution of the cationic surfactant Ethoquad), the drag-reducing effects associated with the presence of an elastic layer are seen to be present over a region increasing in thickness as the velocity

increases, and the better scaling correlation for this type of fluids (3L) is drag reduction versus  $V$ , the correlation that we have recently proposed [1] and shown to be applicable to the majority of drag-reducing fluids reported on in the literature until now (particularly polymer solutions). In the other case (e.g. a solution of nonionic surfactant), the drag-reducing effects are seen across most of the pipe cross-section, even at very low levels of drag reduction. This group of fluids (F-type) scales better according to the  $\tau_w$  versus  $V$  correlation. Only one of the fluids we have tested in our laboratory (nonionic SPE 95285 surfactant) has clearly shown good agreement with this kind of correlation; however, the  $C_{16}TaSal$  surfactant solutions tested in two other experimental studies does also appear to satisfy this kind of scaling.

These two distinct patterns may indicate a different fluid/flow interaction for the two types of drag-reducing fluids. In addition, we also saw some fluids (e.g. a degraded high molecular weight polymer) exhibiting an intermediate behavior, i.e. that did not scale well according to the drag reduction versus  $V$  correlation nor to the  $\tau_w$  versus  $V$  one. It is difficult to ascertain conclusively at this time why some fluids would follow a '3L' pattern, and some others a 'F' one. Based on our results, it seems that, at least for polymers, long molecules may tend to generate 3-layers profiles, while shorter molecules may lean more towards satisfying the  $\tau_w$  versus  $V$  scaling procedure more typical of F-type profiles, but this remains to be proven.

The discussions above pertained mostly to what was previously termed Type A fluids, and it is not yet entirely clear how the temperature profiles of a fluid exhibiting Type B characteristics would differ from those of the 3L and F types defined above. Velocity profile measurements by Escudier et al. [20] for fluids showing Type B friction coefficient characteristics were indeed similar to typical 3-layers models, however. Some of our recent temperature profile measurements [13] showed some slight differences in the slope and thickness of the different regions of the profiles between Types A and B fluids, but only at high concentrations. The issue of the Type B drag reduction will be addressed in details in a future article.

#### 4. Summary and conclusions

In this article we extended our earlier study of the diameter effect to both polymer and surfactant solutions. With respect to the Type A/Type B distinction made earlier, it appears that instead of two distinct types of fluids or of drag reduction, it may perhaps be better to think of two regions of flow/additive interactions reflecting different levels of additive response to the flow, with some fluids in a given pipe exhibiting Type A friction behavior at low Reynolds numbers yet also Type B at high Reynolds numbers. The diameter effect appears to be found only in the region where flow may change the fluid properties (Type A). For Type B drag reduction, we see no true diameter effect after the friction coefficients depart from the asymptote at higher Reynolds numbers, a region of likely constant fluid properties (and, of course, there is no diameter effect in the asymptotic regime either). In the Type B region, not only is the friction dependent only on the Reynolds number, but the data suggest that the drag reduction level becomes also about independent of Reynolds number, in a stronger analogy to Newtonian flow. Type B drag reduction could then be simply interpreted as an extension of Type A drag reduction, and to reflect the region where the fluid properties are no longer affected by turbulence, but not yet by mechanical degradation. True diameter effect would pertain then only to the region where turbulence has a (non-degrading) effect on the fluid properties responsible for the drag reduction.

For Type A, where the fluid properties may still undergo some changes with increasing flow intensity (e.g. with bulk velocity), two types of fluid-flow interactions were found: 3L and F types, each reflecting a different effect of the pipe diameter and turbulent profiles.

Firstly, our earlier scaling procedure (drag reduction versus  $V$ ) appears to work well for most polymer solutions. As we have shown before, this scaling procedure is valid for drag-reducing fluids which exhibit 3-layers velocity profiles. Some surfactant solutions, like the Ethoquad cationic surfactant used in this study, scale also very well with this procedure, and, not surprisingly, we measured similar 3-layers temperature profiles, with spreading of the drag-reducing effects from the wall towards the pipe center as  $V$  increases. We call these fluids 3L-type. We saw that the slope of the elastic layer is about twice that of polymer solutions, however, for both temperature and velocity. In most cases, the temperature and velocity profiles of these surfactant solutions show a separate core region, even for asymptotic levels of drag and heat transfer reductions. The existence of such a core region may not be universal nor fundamental, however, given our observation that the addition of small amounts of  $\text{Cu}(\text{OH})_2$  to a solution of Ethoquad eliminates this region, leading to a constant slope all the way to the pipe center, as in the case of asymptotic polymer solutions, at least at low Reynolds numbers.

Secondly, a nonionic surfactant solution we studied (SPE 95285) scales well with another procedure, namely  $\tau_w$  versus  $V$ . Our temperature profile measurements show a very different type of fluid–flow interactions for this kind of solution. From the very onset of drag reduction, drag-reducing effects are present in the entire cross-section of the pipe. Instead of the growth of an elastic layer, the slope of the profile increases with increasing flow velocity, showing a fan-type evolution of temperature profiles. Our observation that the fan-type temperature profiles are associated with the  $\tau_w$  versus  $V$  scaling procedure is also supported by earlier measurements of velocity profiles.

Finally, another fluid, a highly-concentrated but degraded polymer solutions exhibited scaling that was not correlated as well as the other fluids by either approach, and may well belong to an intermediate category.

Since the two scaling procedures give significantly different results, i.e. fluids which scale well with one procedure show large disagreement with the other (about 30% in terms of drag reduction), we believe that there may be two basic modes of interaction between additive and flow, the distinction between them not simply one between polymer and surfactants. These modes are reflected in very different velocity and temperature profiles, the reasons behind this difference not being known at this time.

On the practical side, it is important to note that we now have available two very good methods for the prediction of the diameter effect for drag-reducing solutions. Adequate predictive scaling is indeed a very important issue for industrial applications, especially those involving very large pipes that cannot readily be studied in the laboratory. Of course, one would have to find out which type of fluid the solution of interest belongs to before choosing the type of correlation to use, but even if the fluid has not yet been reported on in the literature, one could likely make an educated guess, or better still, conduct some simple experiments to determine the type of fluid in question. Hopefully, once this issue will have been studied further, researchers will be able to understand better what flow or fluid characteristic make a fluid belong to one category rather than the other, and perhaps predict this as well.

## Acknowledgements

We acknowledge gratefully the financial support of the California Institute for Energy Efficiency, and of the California Energy Commission (D. Hatfield, program manager) and the generous supply of surfactants by Drs. S. Shapiro and M. Hellsten (AKZO-Nobel Chemicals). GA also wishes to acknowledge the

Universidad Nacional Autonoma de Mexico, and especially the DGAPA and the IIM for support granted through their scholarship program.

## References

- [1] K. Gasljevic, G. Aguilar, E.F. Matthys, An improved diameter scaling correlation for turbulent flow of drag-reducing polymer solutions, *J. Non-Newtonian Fluid Mech.* 84 (2/3) (1999) 131–148.
- [2] P.S. Virk, H.S. Mickley, K.A. Schmitt, The ultimate asymptote and mean flow structure in Toms' phenomenon, *ASME J. Appl. Mech.* 37 (2) (1970) 488–493.
- [3] K. Schmitt, P.O. Brunn, F. Durst, Scaling-up correlations for drag reducing surfactants, in: *Progress and Trends in Rheology II*, 1988, pp. 249–252.
- [4] A. Sood, E. Rhodes, Pipeline scale-up in drag reducing turbulent flow, *Can. J. Chem. Eng.* 76 (1998) 11–18.
- [5] A.V. Shenoy, A review of drag reduction with special reference to micellar systems, *Colloid Polym. Sci.* 262 (1984) 319–337.
- [6] H.W. Bewersdorff, D. Ohlendorf, The behavior of drag-reducing cationic surfactant solutions, *Colloid Polym. Sci.* 266 (1988) 941–953.
- [7] I.L. Povkh, A.V. Stupin, *Turbulent Flows of Solutions of Micelle-Forming Surfactants*, Mechanics of Turbulent Flows, Nauka, Moscow, Russia, 1980, pp. 44–49.
- [8] H.W. Bewersdorff, N.S. Berman, The influence of flow-induced non-Newtonian properties on turbulent drag reduction, *Rheol. Acta* 27 (1988) 130–136.
- [9] H. Usui, T. Itoh, T. Saeki, On pipe diameter effect in surfactant drag-reducing pipe flows, *Rheol. Acta* 37 (1998) 122–128.
- [10] P.S. Virk, D.L. Waggener, Aspects of mechanisms in Type B drag reduction, in: A. Gyr (Ed.), *Structure of Turbulence and Drag Reduction*, IUTAM Symposium, Zurich, Switzerland, 25–28 July, Springer, Berlin, 1989.
- [11] P.S. Virk, D.L. Waggener, The effect of salinity on turbulent drag reduction by polyelectrolyte additives at high Reynolds numbers, in: *Addendum to the Proceedings of the International Symposium on Seawater Drag Reduction*, 22–23 July 1998, Newport, Rhode Island, 1998.
- [12] K. Gasljevic, An experimental investigation of drag-reduction by surfactant solutions and of its implementation in hydronic systems, Ph.D. dissertation, UCSB, April 1995.
- [13] G. Aguilar, An experimental study of drag and heat transfer reductions in turbulent pipe flows for polymer and surfactant solutions, Ph.D. dissertation, UCSB, August 1999.
- [14] S. Rochefort, S. Middleman, Effect of molecular configurations on Xanthan gum drag reduction, in: Y. Rabin (Ed.), *AIP Proceedings Polymer-Flow Workshop*, No. 137, 1985, pp. 117–127.
- [15] J.L. Zakin, J. Myska, Z. Chara, New limiting drag reduction and velocity profile asymptotes for nonpolymeric additives systems, *AIChE J.* 42 (12) (1996) 3544–3546.
- [16] K. Gasljevic, E.F. Matthys, Experimental investigation of thermal and hydrodynamic development regions for drag-reducing surfactant solutions, *J. Heat Transfer* 119 (1) (1997) 80–88.
- [17] G. Aguilar, K. Gasljevic, E.F. Matthys, Coupling between heat and momentum transfer mechanisms for drag-reducing polymer and surfactant solutions, *J. Heat Transfer* 121 (4) (1999) 796–802.
- [18] J. Myska, J.L. Zakin, Comparison of flow behaviors of polymeric and cationic surfactant drag reducing additives, in: *Proceedings of the 1996 ASME Fluids Engineering Division Summer Meeting*, ASME Publication, Vol. FED 237, No. 2, 1996, pp. 165–168.
- [19] Z. Chara, J.L. Zakin, M. Severs, J. Myska, Turbulence measurements of drag-reducing surfactant systems, *Exp. Fluids* 16 (1993) 36–41.
- [20] M.P. Escudier, F. Presti, S. Smith, Drag reduction in turbulent pipe flow of polymers, *J. Non-Newtonian Fluid Mech.* 81 (1999) 197–213.
- [21] G.-C. Liaw, J.L. Zakin, G.K. Patterson, Effects of molecular characteristics of polymers on drag reduction, *AIChE J.* 17 (2) (1971) 391–397.
- [22] M. Hellsten, I. Harwigsson, US Patent No. 5,339,855 and Swedish Patent No. 502,764, 1996.
- [23] M. Ollis, The scaling of drag-reducing turbulent pipe flow, Ph.D. dissertation, University of Bristol, 1981.